



## SYNTHESIS AND ELECTRICAL PROPERTIES OF COBALT SUBSTITUTED Y-TYPE CALCIUM HEXAFERRITES

S. B. Lengule<sup>1\*</sup>, P. R. Moharkar<sup>1</sup>, S. R. Gawali<sup>2</sup>, K. G. Rewatkar<sup>3</sup>

<sup>1</sup>A.C.S. College, Tukum, Chandrapur, (M.S.), India (442401)

<sup>2</sup>Dr. Ambedkar College, Chandrapur, (M.S.), India (442401)

<sup>3</sup>Dr. Ambedkar College, Nagpur, (M.S.), India (440010)

e-mail: slengule2@gmail.com

### Abstract:

The series of samples of cobalt substituted calcium hexaferrite with composition  $\text{Ca}_2\text{Zn}_2\text{Fe}_{12-x}\text{Co}_x\text{O}_{22}$  where  $x$  varies from 0 to 1 were synthesized by microwave induced sol-gel auto-combustion route. X-ray diffraction patterns of all prepared samples manifests that the synthesized samples has single phase Y-type hexagonal crystal structure. The influence of substitution of  $\text{Co}^{3+}$  ion for  $\text{Fe}^{3+}$  ion on the lattice constants, cell volume, X-ray density, bulk density and porosity of samples has been studied. The DC electrical conductivity of the samples were measured as a function of temperature from 300 K to 873 K using two probe techniques. The phenomenon of conduction was explained on the basis of a Verwey hopping model.

**Key words:** Y-type hexagonal ferrite, Structural property, Electrical property, Sol-gel auto-combustion route.

### Introduction:

Hexagonal ferrites has attracted much attention for technological applications in wide range of frequencies. The electrical and magnetic properties make hexaferrites one of the important materials today [1,2]. The hexaferrites have a very good magnetic and dielectric properties that depend on several factors such as processing condition, sintering temperature and time, chemical composition and substitution of different cations [3-5]. The hexaferrites have been classified according to structure into six main classes: M-type, Y-type, W-type, Z-type, X-type and U-type. Y-type ferrite is a very useful in radar satellite, radar absorbing paint, industrial heaters, dryers multiplier chip inductors, LC filters and high power microwave devices [6]. Recently, Y-type ferrite fibres have been reported as a part of development of ceramic fibre [7].

In current research, the samples of Y-type cobalt substituted calcium hexaferrite have been synthesized by microwave induced sol-gel auto-combustion route. The influence of substitution of  $\text{Co}^{3+}$  ion for  $\text{Fe}^{3+}$  ion on the lattice constants, cell volume, X-ray density, bulk density and porosity of samples have been investigated.

### Experimental:

#### Sample preparations

The starting materials to synthesize cobalt substituted calcium hexaferrite samples with generic formula  $\text{Ca}_2\text{Zn}_2\text{Fe}_{12-x}\text{Co}_x\text{O}_{22}$  are AR grade calcium nitrate, iron nitrate, cobalt nitrate, zinc nitrate and urea. The appropriate amounts of metal nitrates  $\text{Ca}(\text{NO}_3)_2 \cdot 4\text{H}_2\text{O}$ ,  $\text{Fe}(\text{NO}_3)_3 \cdot 9\text{H}_2\text{O}$ ,  $\text{Co}(\text{NO}_3)_2 \cdot 6\text{H}_2\text{O}$  were dissolved in minimum amount of deionized water at the

temperature of 50 °C placed in a beaker. These metal nitrates were used as oxidants. The fuel urea then added into the prepared aqueous solution. The initial composition of solution containing metal nitrates and urea was based on the total oxidizing and reducing valences of the oxidizer and the fuel using the concept of propellant chemistry [8].

The solutions as prepared in beaker were mixed together to form a homogeneous transparent aqueous solution. The aqueous solution was then heated into the micro-wave oven. After few minutes aqueous solution get converted into wet gel by evaporating the water. After the wet gel reaches the point of spontaneous combustion, it begins burning and becomes a solid which burns at a temperature above 1000 °C. The combustion is not completed until all the flammable substances are consumed and the resulting material is a loose, highly friable substance exhibiting voids and pores formed by escaping gases during combustion reaction. The ash of cobalt substituted calcium ferrite was obtained after complete combustion. The ash was then ground in agate mortar and then pressed into pellets using PVA as binder. These pellets were finally annealed at 950 °C for 2 hour at a heating rate of 5 °C/min.

#### Characterization

The phase identification of samples were carried out by using a Philips X-ray diffractometer (PW-1710) and Cu-K $\alpha$  radiation with the wavelength  $\lambda = 1.54056 \text{ \AA}$ . The X-ray pattern showed the formation of a single phase of Y-type hexagonal ferrite without any impurity.

The values of lattice parameters  $a$  and  $c$  and the unit cell volume  $V$  were calculated by using following equations.

$$\frac{1}{d^2} = \frac{4(h^2+hk+k^2)}{3a^2} + \frac{l^2}{c^2} \quad (1)$$

where,  $a$  and  $c$  are lattice parameters

$$V = 0.8666a^2c \quad (2)$$

The experimental density (bulk density)  $D$  of the samples was calculated using relation:

$$\text{Density } D = \frac{\text{mass}}{\text{volume}} \quad (\text{gm/cm}^3) \quad (3)$$

where mass of the sample was determined using digital balance and the volume was calculated by measuring the sample dimensions.

The theoretical density (X-ray density)  $D_x$  was calculated from the relation:

$$D_x = \frac{ZM}{N_A V} \quad (\text{gm/cm}^3) \quad (4)$$

where  $Z=3$  is the number of molecules for Y-type hexagonal unit cell,  $M$  is the molar mass,  $N_A = 6.023 \times 10^{23}$  (molecules per mole) is Avogadro's number and  $V$  is the unit cell volume.

The porosity  $P$  is calculated using relation:

$$P = 1 - \frac{D}{D_x} \quad (5)$$

where  $D$  and  $D_x$  are the experimental and theoretical densities respectively.

As these ferrites have very high resistivity, so the four probe method was employed to study DC electrical resistivity of the said ferrites system in the temperature range 300K to 873 K. The DC electrical resistivity of all the samples decreases with

increasing temperature in accordance with Arrhenius equation[6]

$$\rho = \rho_0 \exp\left(\frac{\Delta E}{k_B T}\right) \quad (6)$$

where, ' $k_B$ ' is the Boltzmann constant, ' $T$ ' is temperature and ' $\Delta E$ ' is the activation energy, which is the energy needed to release an electron from the ion for a jump to neighbouring ion, giving rise to the electrical conductivity.

The activation energy of the cobalt substituted calcium hexaferrites have been determined from the slope of plots of  $\ln(\rho)$  versus temperature ( $1000/T$ ) above and below the transition temperature ( $T_1$ ).

## Results and discussion:

### XRD analysis

The XRD patterns of the samples are shown in Fig 1. The crystallographic data are tabulated in Table 1. The XRD data are analyzed by using computer software PCPDF Win, PowderX and FullProf Suite. By comparing the patterns with JCPDS, the phases in the different samples are determined. It is being observed that most of the hexagonal grains are of same size. Using  $2\theta$ , the observed  $d$ -values and intensity calculations,  $d$ -value is recalculated and  $(h k l)$  planes are finalized. The values shown in the Table 2(a) and (b) confirm the formation of single phase Y-type hexagonal ferrites. The lattice parameters  $a$  and  $c$  are found to be 5.0418 and 44.1876 for the sample  $\text{Ca}_2\text{Zn}_2\text{Fe}_{11.5}\text{Co}_{0.5}\text{O}_{22}$  and 5.0274 and 44.0628 for the sample  $\text{Ca}_2\text{Zn}_2\text{Fe}_{11}\text{CoO}_{22}$ . The space group for the samples is observed to be  $R\bar{3}m$  (SG No. 166).

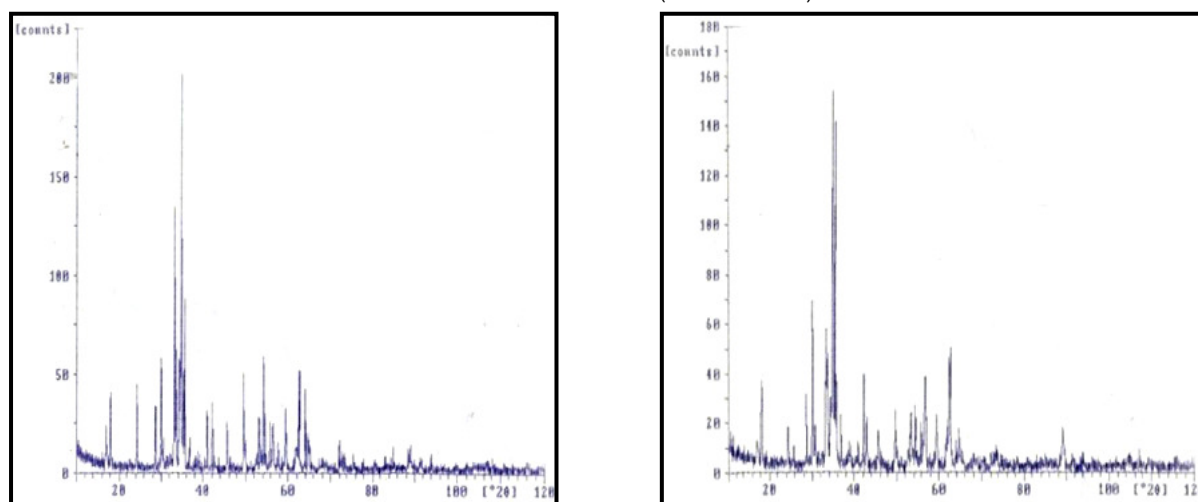


**Fig. 1:** X-ray diffraction spectra (a) Sample  $\text{Ca}_2\text{Zn}_2\text{Fe}_{11.5}\text{Co}_{0.5}\text{O}_{22}$   
(b) Sample  $\text{Ca}_2\text{Zn}_2\text{Fe}_{11}\text{CoO}_{22}$

**Table 1:** Lattice constants a and c, cell volume V, X-ray density D<sub>x</sub>, Bulk density D and Porosity P of cobalt substituted calcium hexaferrite samples.

Sample	a(Å)	c (Å)	V Å <sup>3</sup>	D(gm/cm <sup>2</sup> )	D <sub>x</sub> (gm/cm <sup>3</sup> )	P (%)
Ca <sub>2</sub> Zn <sub>2</sub> Fe <sub>11.5</sub> Co <sub>0.5</sub> O <sub>22</sub>	5.0274	44.0628	1232.32	2.1634	4.2583	49.20
Ca <sub>2</sub> Zn <sub>2</sub> Fe <sub>11</sub> CoO <sub>22</sub>	5.0418	44.1876	1242.93	2.9268	4.2168	30.60

**Table 2:** XRD data (a) Sample Ca<sub>2</sub>Zn<sub>2</sub>Fe<sub>11.5</sub>Co<sub>0.5</sub>O<sub>22</sub> (b) Sample Ca<sub>2</sub>Zn<sub>2</sub>Fe<sub>11</sub>CoO<sub>22</sub>

(a)							(b)						
2θ	d <sub>obs</sub>	d <sub>cal</sub>	I/I <sub>0</sub>	h	k	L	2θ	d <sub>obs</sub> (Å)	d <sub>cal</sub> (Å)	I/I <sub>0</sub>	h	k	l
17.020	5.2182	5.223	8.5	0	0	8	28.280	4.8612	4.8959	20.4	0	0	9
18.150	4.8958	4.909	18.1	0	0	9	24.280	3.6719	3.6719	8.4	0	0	12
24.210	3.6823	3.682	11.5	0	0	12	28.765	3.1288	3.1473	19.0	0	0	14
28.665	3.1194	3.115	15.2	0	0	10	30.085	2.9453	2.9479	42.7	1	0	11
30.035	2.9501	2.956	30.6	1	0	11	30.740	2.9134	2.9375	9.4	0	0	15
33.46	2.6821	2.682	70.0	1	0	13	33.305	2.6946	2.6945	37.6	1	0	13
34.725	2.5876	2.599	100	0	0	17	35.240	2.5579	2.5507	100	1	0	14
35.675	2.5209	2.520	49.3	1	1	0	35.780	2.5137	2.5137	23.4	1	1	0
40.910	2.2096	2.209	15.2	0	0	20	41.035	2.2032	2.2031	5.1	0	0	20
42.010	2.1543	2.159	14.7	2	0	3	42.090	2.1504	2.1534	23.4	2	0	3
45.630	1.9914	1.994	14.1	2	0	9	42.940	2.1097	2.1134	11.5	2	0	5
49.515	1.8439	1.841	27.5	0	0	24	45.750	1.9865	1.9892	7.1	2	0	9
53.290	1.7219	1.712	13.6	2	0	16	49.615	1.8404	1.8360	13.2	0	0	24
54.125	1.6973	1.699	27.5	1	0	26	53.48	1.7162	1.7078	13.2	2	0	16
55.565	1.6567	1.650	15.2	2	1	0	54.240	1.6939	1.6916	13.8	1	0	24
59.325	1.5603	1.564	17.5	2	1	9	55.65	1.6543	1.6568	10.9	1	1	20
62.485	1.4888	1.486	28.3	1	1	24	56.710	1.6259	1.6267	22.6	2	0	18
64.045	1.4563	1.455	18.7	3	0	0	59.320	1.5605	1.5664	12.6	1	1	22
							62.275	1.4833	1.4826	26.6	1	1	24
							64.095	1.4553	1.4583	6.2	3	0	14
							64.590	1.4453	1.4442	10.4	3	0	3

The lattice parameters a and c increases with increase in the concentration of Co<sup>3+</sup> ions as shown in Table 1. The variation in lattice parameter with substitution is indicated of desired changes on crystallographic sites. It also implies that easy magnetized c-axis undergoes little more expansion than a-axis with Co<sup>3+</sup> ions substitution. It is related to larger ionic radii of Co<sup>3+</sup> (0.68Å) than Fe<sup>3+</sup> ion (0.64Å)[9].

The X-ray density varies in the range of 4.2168 to 4.2583 gm/cm<sup>3</sup> and porosity varies 30.60% to 49.20% . It was observed that experimental values of density D (Bulk density) to be in general less than those of D<sub>x</sub> (theoretical density), which was expected due to presence

of unwanted pores created during synthesis process. It was seen that introduction of Co<sup>3+</sup> ions in hexagonal ferrites may affect the grain size development during firing process and decrease the porosity[10]. Thus it can be concluded that substitution enhance the firing process and increase the grain size to leading to decrease of porosity.

**DC conductivity**

Fig. 2 shows the graph of electrical conductivity ln (σ) verses temperature (10<sup>3</sup>/T) for all ferrites sample.

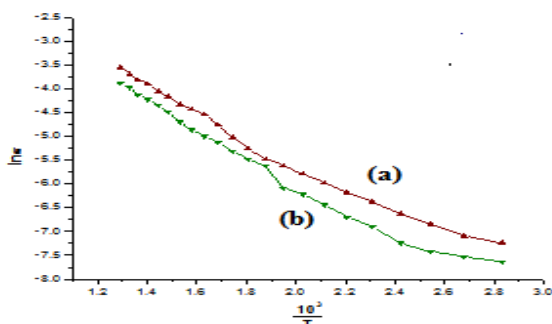


**Fig.2** : Variation of  $\ln(\sigma)$  with temperature ( $10^3/T$ ): (a) Sample  $\text{Ca}_2\text{Zn}_2\text{Fe}_{11.5}\text{Co}_{0.5}\text{O}_{22}$  (b) Sample ( $\text{Ca}_2\text{Zn}_2\text{Fe}_{11}\text{CoO}_{22}$ )

The linearity of conductivity in the graph breaks near the Curie temperature, indicative of two conductivity mechanism with different activation energy are present the ferrite compounds. This break from the linearity at transition temperature ( $T_t$ ) may be assignment to the magnetic order phase transition from ferri to paramagnetic region. The electrical conduction in ferrite can be explained by Verway hopping mechanisms of electrical conductivity accordingly, electronic conduction in ferrites occurs due to hopping of electrons between ions of the same element present in more than one valence state, distributed randomly over crystallographically equivalent lattice sites. The widely studied Y-type hexagonal ferrites, which is structurally represented as (TS) and (TS)\* (TS)\*\*, where S is two oxygen layered block having chemical composition  $\text{Fe}_2^{3+} \text{O}_8^{2-}$ , while T is four layered block having chemical composition  $\text{Ca}_2^+ \text{Fe}_8^{3+} \text{O}_{14}^{2-}$ . The symbol \* indicates rotation of corresponding block through  $120^\circ$ , about the c-axis. In the crystal structure,  $\text{Fe}^{3+}$  ions prefer six crystallographic site  $6c_{vi}^*$ ,  $6c_{iv}$ ,  $6c_{iv}$ ,  $3b_{vi}^*$ ,  $18h_{vi}$  and  $3a_{vi}$ . out of these six position,  $6c_{vi}^*$  and  $6c_{iv}$  are tetrahedral, while  $6c_{iv}$ ,  $3b_{vi}^*$ ,  $18h_{vi}$  and  $3a_{vi}$  are octahedral. Oxygen ions occupy 6c and 18h sites [11] Co ions prefix  $3a_{vi}$ ,  $18h_{vi}$  and  $3b_{vi}$  sites [12]. The octahedral-octahedral hopping is the dominant mode of conduction as distance between two metal ions at octahedral sites are smaller than distance between metal ions at tetrahedral and octahedral sites, tetrahedral-tetrahedral hopping is ignored for the reason that small amount of  $\text{Fe}^{2+}$  ions formed during materials synthesis which occupy only octahedral sites. Hence conduction may be taken to be the electronic hopping between  $\text{Fe}^{3+}$  ions and  $\text{Fe}^{2+}$  ions at octahedral sites.

The room temperature resistivity of the ferrites compounds at room temperature for all the samples of the series is enumerated in Table 3 and are in the range of 23.8 to 30.8

$\text{M}\Omega\text{-cm}$ . The substituted  $\text{Co}^{3+}$  ions occupy  $\text{Fe}^{3+}$  ions position preferable in octahedral sites [13]. As the content of  $\text{Co}^{3+}$  ions increases there is a decrease in the  $\text{Fe}^{3+}$  ions in octahedral sites. The number of  $\text{Fe}^{2+}$  ions formed also decreases as this depends on the content of  $\text{Fe}^{3+}$  ions. This reduces the hopping electrons between  $\text{Fe}^{3+}$  and  $\text{Fe}^{2+}$  ions, resulting in increase of resistance, but in the present series, it is seen that resistance decreases with substitution of dopent, it may due to the face that addition of  $\text{Co}^{3+}$  ions may be converted to  $\text{Co}^{2+}$  and vice-versa [14].

The activation energies in case of  $\text{Ca}_2\text{Zn}_2\text{Fe}_{12-x}\text{Co}_x\text{O}_{22}$  ferrite have been constructed from the slopes of plots of electrical conductivity versus temperature above and below the transition temperature ( $T_t$ ) and are given in Table 3. By increasing substitution about of  $\text{Co}^{3+}$  ions, the activation energy decreases from 0.32 to 0.31 eV in paramagnetic region and from 0.23 to 0.21 eV in ferrimagnetic region. It can also be seen than the activation energy in the paramagnetic region is higher than that of ferrimagnetic region. There are several factors for such a variation in activation energy such as change in resistivity including the formation of other secondary phases and change in porosity of the samples. The decrease in porosity causes slight loose packing between the grains. The loose packing could have less retarding force on charge carriers which may lead to help in conduction of free electrons from grain to grain.

### Conclusion:

The cobalt substituted calcium hexaferrite samples were synthesized by the microwave induced sol-gel auto-combustion route. The XRD data have confirm the formation of single Phase Y-type hexaferrites and the values of a and c of the sample supports this confirmation. The synthesized samples are semiconductors. The dc electrical resistivity as well as activation energy ( $E$ ) decreases with increasing concentration of  $\text{Co}^{3+}$  ions. The phenomenon of conduction in the prepared samples was explained on the basis of a Vervey hopping mechanism.

### Acknowledgement:

Authors are grateful to Principal, Dr. Ambedkar College, Deekshabhoomi, Nagpur for giving us permission to use laboratory facility. The authors are also thankful to Dr. V. M. Nanoti, Dean Academics, Priyadarshini College of Engineering, Nagpur for motivation.

**Table 3 :** Electrical resistivity and activation energy in Para and Ferri magnetic regions of cobalt substituted calcium ferrite.

Sample	Room Temperature Resistivity $\rho(\text{M}\Omega\text{-cm})$	Activation Energy $\Delta E$ (eV)		Trans. temp. $T_t$ (K)
		Ferri	Para	
$\text{Ca}_2\text{Zn}_2\text{Fe}_{11.5}\text{Co}_{0.5}\text{O}_{22}$	30.3	0.23	0.32	594
$\text{Ca}_2\text{Zn}_2\text{Fe}_{11}\text{CoO}_{22}$	23.8	0.21	0.31	533

**References:**

- [1] R. M. Almeida, W. Paraguassu, D. S. Pires, R. R. Correa, C. W. A. Paschoal, *Ceram. Int.* 35 (2009) 2443-2447.
- [2] Y. Bai, J. Zhou, Z. Gui, Z. Yue, L. Li, *Mater. Sci. Eng. B* 99 (2003) 266-269.
- [3] X. Wang, D. Li, L. Lu, X. Wang, J. *Alloys Compd.* 273 (1996) 45.
- [4] M. A. Ahmed, N. Okasha, R. M. Kershi, *J. Magn. Magn. Mater.* 320(2008)1146-1150.
- [5] Y. Bay, F. Xu, L. Qiao, J. Zhou, J. *Alloys Compd.* 473 (2009) 505-508.
- [6] G. Winkler, H. Dotsch, *Pro. 9<sup>th</sup> Europ. Microwave Conf. Brighton*, (1979) 13.
- [7] R. C. Puller, S. G. Appleton, M. H. Stacky, M. D. Tayler, A. K. Bhattacharya, J. *Magn. Magn. Mater.* 186 (1998) 313.
- [8] Jain S. R., Adiga K. C. and Pai Verneker V. R., *Combustion Flame*, 40 (1981) 71-79.
- [9] T. M. Meaz, C. B. Koch, *Hyp Interact.*, 156/157(2004) 341-346.
- [10] D. M. Hemed, O. M. Hemed, *American Journal of Applied Science* 5(4) (2008) 289-295.
- [11] S. G. Lee, S. J. Kwon, *J. Magn. Magn. Mater.* 153 (1996) 181.
- [12] G. H. Jonker, J. H. Vann Santen, *Physics*, 16 (1954) 337.
- [13] P. Beuzelen, P. Feldman, W. Simonet, *IEEE Transition on Magnetics* 173, (1981)135.
- [14] I. Soiban, S. Phanjouban, H. B. Sharma, H.H.K. Sharma, Chandra Prakash, *Indian J. Phys.* 83(3) (2009) 285-290.